CSCE Annual Conference

Growing with youth – Croître avec les jeunes

Laval (Greater Montreal)

June 12 - 15, 2019

EFFECT OF SLENDERNESS RATIO ON THE PERFORMANCE OF CONCRETE COLUMNS REINFORCED WITH GFRP BARS AND SPIRALS

Waseem Abdelazim[1], Hamdy M. Mohamed[1], and Brahim Benmokrane[1]
[1] Department of Civil Engineering, Université de Sherbrooke, Sherbrooke, Quebec, Canada.

ABSTRACT: This study is a part of an ongoing research program at the University of Sherbrooke that aims to investigate the structural performance of Fiber Reinforced Polymers (FRP)-Reinforced Concrete (RC) columns. This paper presents test results of an experimental program to describe the behavior of circular concrete columns reinforced with glass-FRP (GFRP) bars and spirals subjected to concentric loading. The 305 mm diameter columns were designed according to CAN/CSA S806-12 code requirements. The study was conducted to investigate the effect of slenderness ratio on the performance and axial capacity of GFRP-RC columns. In addition, the study aimed at providing basic technical information and yielding better understanding of the concentric behavior of circular GFRP reinforced with different slenderness ratios. Test results are presented in terms of axial load capacity, axial and lateral deformation, strain behavior of GFRP bars and spirals. Test results showed the significant contribution of GFRP reinforcement to resisting the applied compression loads over the tested range of slenderness ratios.

1. INTRODUCTION

Design Codes have not yet addressed stability and buckling issues related to slender concrete columns reinforced with fiber-reinforced polymer (FRP) bars owing to a lack of experimental data. Columns are defined as slender if they experience buckling at loading levels lower than that of short or stocky columns that fail without undergoing any noticeable lateral deformations. CSA S806-12 allows the use of FRP reinforcement in short columns and conservatively ignores the contribution of FRP bars in compression. Moreover, CSA S806-12 classifies GFRP-RC columns are short or long, relying on the ACI 318 slenderness limit for steel-RC columns, disregarding that FRP-reinforced members reinforced with FRP might resist buckling instability differently than steel-reinforced ones.

Over the last two decades, valuable extensive experimental and analytical research have been conducted to establish the behavior of concrete columns internally reinforced with FRP bars considering a wide range of parameters (De Luca et al. 2010; Tobbi et al. 2012; Pantalides et al. 2013; Afifi et al. 2014; Mohamed et al. 2014; Hadi et al. 2016; Hadhood et al. 2017a, b, and c; Guérin et al. 2018; Sheikh and Kharal 2018). Most of the experimental programs found in literature were performed for short columns and, therefore, the second-order effects due to buckling problems were excluded.

Few studies have investigated the stability of slender FRP-RC compression members. Mirmiran et al. (2001) developed an analytical model to study the behavior of slender FRP-RC columns. The model was verified with steel-RC columns from the literature. Mirmiran et al. (2001) recommended reducing the slenderness limit of 22 for steel-RC columns to 17 for FRP-RC columns with a reinforcement ratio of 1%. Zadeh and Nanni (2017) applied a theoretical derivation for the slenderness limits of FRP-RC columns with a rectangular cross section. The contribution of FRP bars in compression was limited to the concrete

compressive strength. The suggested slenderness limits were 14 and 19 for GFRP-RC and CFRP-RC columns bent in a single curvature, respectively. Hals et al. (2016) evaluated the behavior of slender (λ = 49) high-strength-concrete columns (concrete compressive strength of 90 MPa) reinforced with GFRP bars under eccentric and concentric loading. The short and slender columns had various loading conditions, so that the reduction in loading capacity due to slenderness variations could not be observed. Recently, Xue et al. (2018) conducted concentric and eccentric loading tests on slender (λ varied from 20.8 to 41.6) rectangular GFRP-RC columns. They concluded that all tested columns exhibited concrete-crushing failure with no rupture of the FRP bars. Moreover, the experimental research on slender FRP-RC columns is very limited, which accentuates the need for more experimental studies that investigate the performance of slender FRP-RC columns.

2. EXPERIMENTAL PROGRAM

2.1 Test Parameters and Column Design

A total of 5 full-scale circular concrete columns with GFRP reinforcement were prepared and tested under monotonic static concentrically axial loading. All of the columns were 305 mm in diameter. The experimental program investigated the behavior of slender GFRP-RC columns with the slenderness ratio. Herein, the slenderness ratio, $\lambda = kL/r$, is expressed in terms of the unsupported length of the column (L); the effective length factor, k; and the radius of gyration of its cross section, r. The test setup was designed to achieve an effective length factor k equal to unity, as explained below. Five different heights were selected to cover a wide range of column slenderness ratios (14, 17, 23, 26, and 33).

Two main boundary conditions determine the design of longitudinal reinforcement: the total number of bars and bar diameter. If the number of longitudinal bars in any circular column is less than eight, bar orientation may significantly affect the bending strength of the loaded column and should be considered in the column analysis (ACI 318-14). Although all test specimens are loaded concentrically, there are second-order bending moments due to the expected lateral buckling. Hence, and to eliminate the test complexity, a minimum of eight equally spaced bars were used for each column. On the other hand, CSA S806-12 stipulates that the minimum bar diameter for longitudinal FRP bars shall not less than 15 mm. Therefore, consistent with code recommendations, the longitudinal reinforcement was decided to be 8 No. 5 (2.19%). All GFRP spirals were designed according to CSA S806-12 to provide thorough confinement so as to avoid buckling of the GFRP longitudinal bars. All columns were reinforced in the transverse direction with No. 3 continuous spirals without any lapped splices. Figure 1 shows the reinforcement details. The details for the 5 specimens were indicated in Table 1.

Table 1: Test matrix, specimens details, and test results

Specimen ID	Geometry*		Longitudinal Reinforcement		Transverse Reinforcement			P_{peak}	P_{peak} / $(f'_c A_g)$
	L (mm)	λ	ρ_L (%)	Number of bars	ρ_T (%)	Bar size	Pitch (mm)	(kN)	
C1	1000	14						3,535	1.04
C2	1250	17						3,490	1.02
C3	1750	23	2.19	8 No. 5	1.17	No. 3	80	3,453	1.01
C4	2000	26						3,359	0.99
C5	2500	33						3,331	0.98

* All columns are 305 mm in diameter.

2.2 Materials and Specimen Production

All reinforcing cages were assembled and fabricated in the laboratory of materials and structures of the University of Sherbrooke (Sherbrooke, Quebec, Canada). The GFRP bars and spirals used were sand coated and manufactured by a pultrusion process using continuous glass fibers impregnated in a thermosetting vinyl-ester resin (see Figure 1). One size of GFRP bars with an average fiber content of 83.8% were used as longitudinal reinforcement (No. 5), while all the GFRP-RC columns were transversally reinforced with No. 3 GFRP spirals. The average ultimate longitudinal tensile properties of the GFRP materials were provided by the manufacturer and were determined according to CSA S806-12 (Annex C), as reported in Table 2. The bars and spirals were tightly connected with cable ties to avoid self-twisting and to ensure cage verticality, as shown in Figure 2.

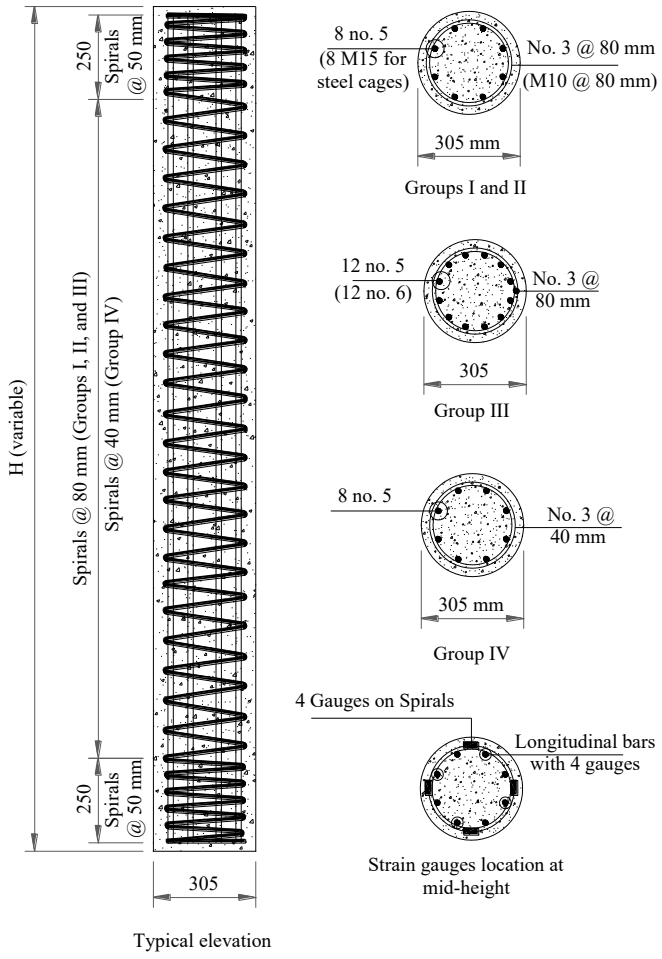

Figure 1: Typical layout, reinforcement details, and internal instrumentation.

A single batch of ready-mixed normal-strength, normal-weight concrete with a maximum aggregate size of 10 mm was used to cast all the columns in an upright position. The average concrete compressive strength was determined based on testing nine 100 mm x 200 mm. standard concrete cylinders cured under the same conditions as the column specimens. Concrete cylinders were tested on the same day as the start of testing of the column specimens. The measured average concrete compressive strength used in the analysis was 46.6 MPa.

Table 2: Mechanical and physical properties of the GFRP reinforcement

Bar Size	Diameter (mm)	Area [1] (mm^2)	Fiber Content (%)	Elastic Tensile Modulus [2] (GPa)	Nominal Tensile Strength (MPa)	Tensile Strain (%)
# 3 (spiral)	9.5	71	78.9	51.1	1281	2.51
# 5	15.9	200	83.6	61.8	1449	2.35

[1] Nominal area.

[2] Average ultimate longitudinal tensile properties as provided by the manufacturer; test method CSA S806 Annex C.

(a)

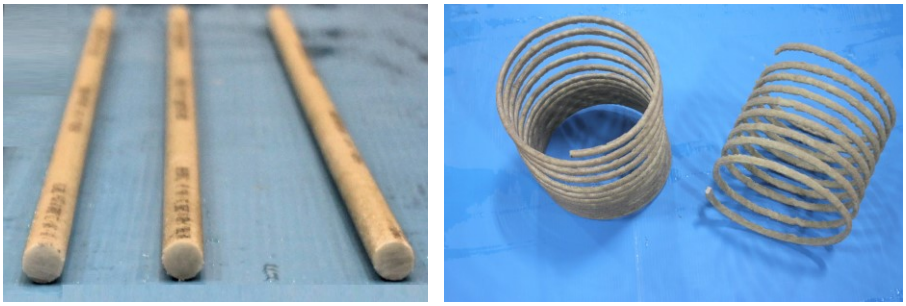

(b)

Figure 2: (a) Assembly of GFRP cages; (b) samples of the GFRP bars and spirals.

2.3 Instrumentation and test setup

All specimens were instrumented to measure the axial and lateral deformations as well as the local strains in the longitudinal bars, spirals, and concrete surface. All of the strain gauges were located at the mid-height of the columns, where the maximum strain values are expected. Strain gauges on concrete face, bars, and spirals were installed on the outermost locations on opposite sides defining the expected concave and convex faces of the columns as they deform. The column's horizontal deflection was gauged with three LPOTs mounted horizontally at column mid- and quarter-heights.

Prior to testing, both ends of each column were capped with a thin perfectly self-leveling layer of high-strength cementitious grout to achieve uniform distribution of the applied loads. Two identical rigid steel collars were designed to confine the top and bottom zones of the tested specimens to prevent any premature local failure. The axial load was applied with a knife-edge pattern to replicate the case of a perfect pin-ended column, $k = 1$ (see Figure 3). The column specimens were tested with an 11400 kN MTS testing machine. All columns were loaded up-to a level of 75% of the estimated capacity under loading control at a constantly increasing rate of 2.5 kN/s. Testing continued under displacement control at a displacement rate of 0.002 mm/s until the specimens could not withstand the applied axial force or the longitudinal GFRP bars ruptured.

Figure 3: Test setup.

3. ANALYSIS OF EXPERIMENTAL RESULTS

3.1 Failure Modes

The failure modes of all the columns could be broken down into two main stages. Stage one is represented by concrete rupture initiated by gradual cover spalling accompanied with a significant reduction in the load-carrying capacity of the tested column. Prior to cover spalling, vertical cracks started to initiate at an average load level of approximately 90% of the achieved maximum load. These cracks rapidly widened and propagated, causing the concrete cover to spall off the concrete core. In general, the slender GFRP-RC

columns lost more load-carrying capacity after the initial spalling of the concrete cover. For example, GFRP-RC columns C1 (considered a short column) and C5 (considered a long column) lost around 20% and 40%, respectively, of their maximum bearing capacity after the concrete cover had completely spalled off.

The second failure stage of the column corresponds to the rupture of the core components (transversal spirals, longitudinal bars, and concrete core). In addition to separation of the concrete cover, the concrete core started to dilate, causing a passive confining pressure of the spirals. The recorded tensile strains of the GFRP spirals at the peak loads ranged from 700 to 1,600 $\mu\varepsilon$ (3% to 6.4% of the ultimate spiral tensile strains). After the peak load, the GFRP spirals confined the concrete core of the column to recover the load drop due to the concrete cover spalling and to enhance the column's ability to experience higher lateral deformations. The test results indicated that all the tested columns experienced no second-peak load. Figure 4 shows the predominant material failure modes of the GFRP-reinforced columns, as outlined above.

During test After test During test After test

Column C1 Column C5

Figure 4: Typical material failure modes

3.2 Loading capacity and axial deformations

Figure 5 depicts the axial stress–axial strain relationship of the tested columns. As expected, the elastic stress–strain diagram was linear during the initial loading state and up-to around 85% of the maximum peak load. Furthermore, all measured concrete strains at the peak loads exceeded the theoretical values of ε_o, where ε_o is the concrete strain corresponding to the maximum concrete compressive strength and ranges from 1,900 to 2,500 $\mu\varepsilon$ for normal-strength concrete (Popovics 1973). Overall, the effect of column slenderness on the concrete strains at peak was very limited and not observed. On the other hand, the average recorded compressive bar strain at the maximum load-bearing capacity was 3,240 $\mu\varepsilon$ (14% of the ultimate tensile GFRP-bar strain). The compression contribution of the GFRP bars was around 11% of the column ultimate bearing capacity. The GFRP reinforcing bars did not exhibit any compression failure up-to peak load.

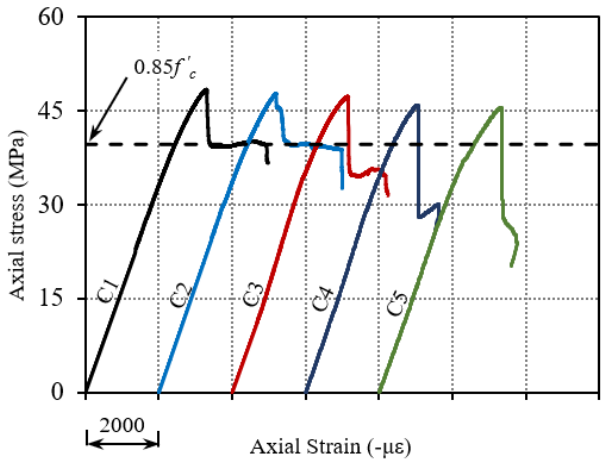

Figure 5: Axial stress-axial strain relationship

Table 1 summarizes the experimental ultimate axial bearing capacity of all tested columns. Columns S-23 and S-33 respectively reached axial compression loads of 3,866 kN (869 kips) and 3,627 kN (815 kips), which are, on average, 9.5% higher than their counterpart columns C3 and C5. Column C1 sustained a maximum compressive load of 3,535 kN (795 kips) which is 1.3%, 2.3%, 5.2%, and 5.8% higher than columns C2, C3, C4, and C5, respectively (Figure 6).

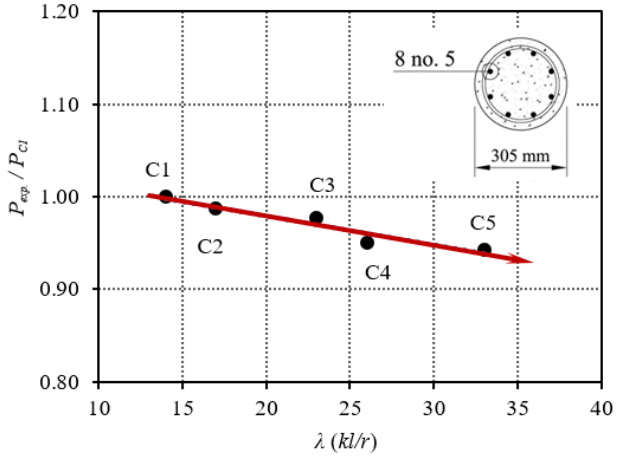

Figure 6: Effect of slenderness ratio on the column axial capacity

Degradation of the peak load could also be used as an index for the impact of additional second-order induced stresses on column-bearing capacity. This confirms an inverse relationship between the ultimate strength of the GFRP-RC columns and column slenderness. In the case of concentrically loaded GFRP-RC columns, however, the effect of slenderness on column axial-bearing capacity could be experimentally concluded as limited and not significant over the studied range of slenderness ratios ranges from λ = 14 to λ = 23.

3.3 Instability buckling load

Perfectly axially-loaded columns that have no initial imperfections with zero-eccentricity loading tend to deflect laterally under a specific load levels called instability buckling loads. The induced second-order deformations or load-delta (*P-δ*) effects create additional nonlinear second-order moments which, in turn, produce additional stresses on the column cross section, which inevitably reduces the column's compressive strength. Experimentally, *P-δ* effects could be observed in terms of the lateral displacement response of the column to the peak and post-peak loads (Figure 7). Overall, none of the columns experienced any instability deformations near to 75% of the ultimate capacity (P_{max}). After that limit, and since the stress distribution was not perfectly uniform due to initial imperfections or unsymmetrical initiation of internal cracks, the irregular stress distribution over the column cross section induced column buckling. Once buckling started, column slenderness controlled the maximum lateral buckling response to peak and post-peak loads. All columns buckled into a single-curvature deformed shape with concave and convex faces. Once the applied loads had been removed at the end of testing, all the GFRP-RC columns returned to a shape similar to that prior to loading state. This confirms the fact that FRP exhibits linear elastic behavior up-to failure.

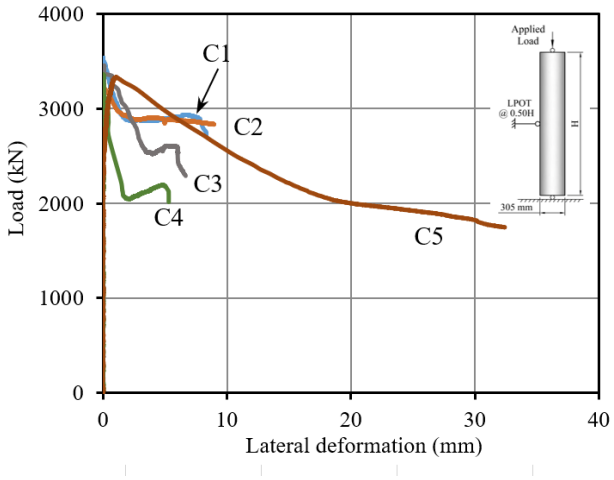

Figure 7: Axial load-lateral deformation response

To sum up, the slender GFRP-RC columns under concentric loads experienced a material-type failure similar to that of the short ones with insignificant effect on column stability up-to ultimate load. The material-failure mode consisted of compressive failure of the concrete, tensile rupture of the GFRP spirals, and compressive rupture of the longitudinal GFRP bars. In addition, using GFRP bars as internal reinforcement in short and slender RC columns significantly contributed to the column bearing capacity.

4. Conclusions

The effect of slenderness on GFRP-RC columns subjected to uniaxial compression loads was investigated using 12 full-scale pin-ended columns with slenderness ratios of 14, 17, 23, 26, and 33. The main concluding remarks are as follows:

1. The failure of both the short and slender GFRP-RC columns was dominated by a material-type failure in terms of gradual concrete cover spalling at peak. Beyond peak, tensile rupture of GFRP spirals, compression rupture of GFRP bars, and buckling of steel bars were observed at ultimate stages.
2. The GFRP reinforcement significantly contributed to resisting the applied compression loads at all slenderness ratios tested from $\lambda = 14$ to $\lambda = 33$. In comparison to the short-column control specimens $\lambda = 14$, the slender columns lost 1.3%, 2.3%, 5.2%, and 5.8% of their strength at slenderness ratios of $\lambda = 17$, $\lambda = 23$, $\lambda = 26$, and $\lambda = 33$, respectively.
3. The instability of FRP-RC columns was experimentally investigated in terms of column lateral displacement and was observed at 75% of the column capacity with an ultimate lateral response measured 1% of the column size. The experimental second-order moments were limited and not significant over the range of slenderness ratios studied ($\lambda = 14$ to $\lambda = 23$).

5. ACKNOWLEDGEMENTS

This research was conducted with funding from the Tier-1 Canada Research Chair in Advanced Composite Materials for Civil Structures, the Natural Sciences and Engineering Research Council of Canada (NSERC), Mathematics of Information Technology and Complex Systems (MITACS), and the Fonds de recherche du Québec en nature et technologies (FRQ-NT). The authors thank the technical staff of the CFI structural laboratory in the Department of Civil Engineering at the University of Sherbrooke. The authors are grateful to Marc Demers, Steven MacEachern, and Jérôme Lacroix for their valuable contributions to testing.

6. REFERENCES

ACI Committee 318, 2014, “Building Code Requirements for Structural Concrete (ACI 318-14) and Commentary (318R-14),” American Concrete Institute, Farmington Hills, MI, 519 pp.

Afifi, M. Z.; Mohamed, H. M.; and Benmokrane, B, 2014, “Axial capacity of circular concrete columns reinforced with GFRP bars and spirals,” *Journal of Composites for Construction*, ASCE, V. 18, No. 1, Feb., p. 04013017.

Canadian Standards Association (CSA), 2012, “Design and construction of building components with fiber reinforced polymers,” CAN/CSAS806-12, Mississauga, Ontario, Canada, 198 pp.

De Luca, A.; Matta, F.; and Nanni, A., 2010, “Behavior of Full-Scale Glass Fiber-Reinforced Polymer Reinforced Concrete Columns under Axial Load,” *ACI Structural Journal*, V. 107, No. 5, Sept.-Oct., pp. 589-596.

Guérin, M.; Mohamed, H. M.; Benmokrane, B.; Shield, C. K.; and Nanni, A., 2018, “Effect of Glass Fiber-Reinforced Polymer Reinforcement Ratio on Axial-Flexural Strength of Reinforced Concrete Columns,” *ACI Structural Journal*, V. 115, No. 4, July, pp. 1049-1061.

Hadhood, A.; Mohamed, H. M.; and Benmokrane, B., 2017a, “Axial load-moment interaction diagram of circular concrete columns reinforced with CFRP bars and spirals: Experimental and theoretical investigations,” *Journal of Composites for Construction*, ASCE, V. 21, No. 2, Jan., p. 04016092.

Hadhood, A.; Mohamed, H. M.; and Benmokrane, B., 2017b, “Experimental study of circular high-strength concrete columns reinforced with GFRP bars and spirals under concentric and eccentric loading,” *Journal of Composites for Construction*, ASCE, V. 21, No. 2, Jan., p. 04016078.

Hadhood, A.; Mohamed, H. M.; Ghrib, F.; and Benmokrane, B., 2017c, “Efficiency of glass-fiber reinforced-polymer (GFRP) discrete hoops and bars in concrete columns under combined axial and flexural loads,” *Composites Part B: Engineering*, V. 114, No. 6, pp. 223–236.

Hadi, M. N.; Karim, H.; and Sheikh, M. N., 2016, “Experimental Investigations on Circular Concrete Columns Reinforced with GFRP Bars and Helices under Different Loading Conditions,” *Journal of Composites for Construction*, ASCE, V. 20, No. 4, 04016009. doi: 10.1061/(ASCE)CC.1943-5614.0000670

Hales, T. A.; Pantelides, C. P.; and Reaveley, L. D., 2016, “Experimental evaluation of slender high-strength concrete columns with GFRP and hybrid reinforcement,” *Journal of Composites for Construction*, ASCE, V. 20, No. 6, Dec., p. 04016050.

Mirmiran, A.; Yuan, W.; and Chen, X., 2001, “Design for Slenderness in Concrete Columns Internally Reinforced with Fiber-Reinforced Polymer Bars,” *ACI Structural Journal*, V. 98, No. 1, Jan.-Feb., pp. 116-125.

Mohamed, H. M.; Afifi, M. Z.; and Benmokrane, B., 2014, “Performance evaluation of concrete columns reinforced longitudinally with FRP bars and confined with FRP hoops and spirals under axial load,” *Journal of Bridge Engineering*, Vol. 19, No. 7, June, p. 04014020.

Pantelides, C. P.; Gibbons, M. E.; and Reaveley, L. D., 2013, “Axial load behavior of concrete columns confined with GFRP spirals,” *Journal of Composites for Construction*, ASCE, V. 17, No. 3, June, pp. 305–313.

Popovics, S., 1973, “A Numerical Approach to the Complete Stress-Strain Curve of Concrete,” *Cement and Concrete Research*, V. 3, No. 5, Sep., pp. 583-599.

Sheikh, S.A.; Kharal, Z., 2018, “Replacement of Steel with GFRP for Sustainable Reinforced Concrete,” *Construction and Building Materials*, V. 160, pp. 767-774.

Tobbi, H.; Farghaly, A. S.; and Benmokrane, B., 2012, “Concrete Columns Reinforced Longitudinally and Transversally with GFRP Bars,” *ACI Structural Journal*, V. 109, No. 4, July-Aug., pp. 551-558.

Xue, W.; Peng, F.; and Fang, Z, 2018, "Behavior and Design of Slender Rectangular Concrete Columns Longitudinally Reinforced with Fiber-Reinforced Polymer Bars," *ACI Structural Journal*, Vol. 115, No, 2, Mar., pp. 311-322.

Zadeh, H. J.; and Nanni, A., 2017, “Flexural Stiffness and Second-Order Effects in Fiber-Reinforced Polymer-Reinforced Concrete Frames,” *ACI Structural Journal*, V. 114, No. 2, Mar.-Apr., pp. 533-544.